

Menooa Avrand

Project Portfolio

(818) 688-1064 | menooaavrand@berkeley.edu | menooaavrand.com

Table of Contents

CalSol - UC Berkeley Solar Vehicle team

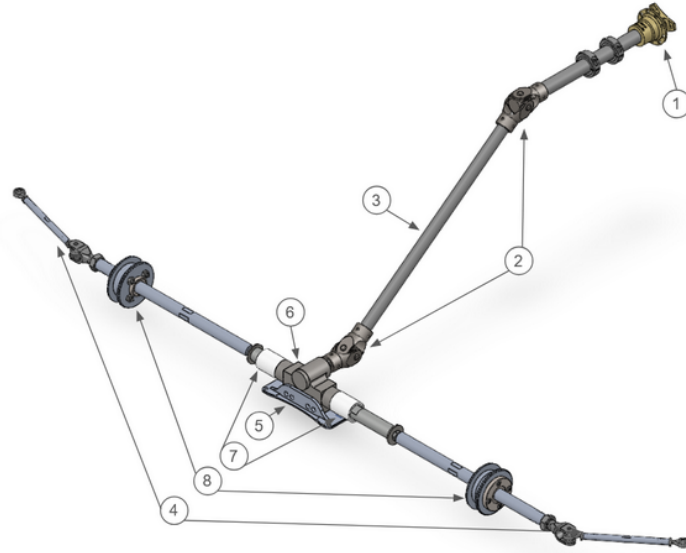
1. Gen 11 Steering System.....	2
2. Vehicle Stability Analysis Tool.....	4
3. Bolt Preload Calculator/Tutorial.....	6

Personal Projects

4. πRo-Bot: Autonomous Fire Suppression Robot.....	8
5. Thermal Paste Performance Evaluation for HT Optimization.....	9
6. 3D Printed Wind Turbine Design and Testing.....	10
7. Microfluidic Exhaust Valve (MUMPS).....	11
8. Assistive Utensil Device.....	12
9. SolarSync: Automated Window Blinds.....	13

1. Gen 11 Steering System

Detailed Critical Design Review Slidedeck



Objective

Designed, engineered, and validated the complete steering architecture for CalSol's 11th-generation solar vehicle, optimizing for safety, rigidity, steering precision, manufacturability, and seamless integration with suspension geometry. The system balances turning performance, structural robustness, anti-bump behavior, and lightweight design to meet our goal/regulation constraints.

Methodology

Developed the steering system using a requirements-driven engineering workflow:

Vehicle Kinematics & Requirements Definition:

Ensured compliance with Ackermann steering geometry while achieving a 7.5 m turning radius ([ASC regulation](#)), limiting wheel steering angles to under 25°, maintaining steering wheel < 500° lock to lock, and preserving anti-bump dictated by front suspension a-arm + tie rod geometry.

PowerSketch Geometry Derivation:

Used SolidWorks sketching to define linkage relationships, solve rack travel, steering axis alignment, tie-rod positioning, and steering knuckle offsets. Final tie-rod length constrained to 6.83 in, defining steering knuckle X-offset of 3.18 in, with optimized Y-offset of 3.8 in to avoid upright interference and reduce rack travel.

Structural Design & FEA Validation:

Simulated for worst-case curb impact steering load based on driver torque → resulting ~7878 N tie-rod load, then performed full-system component analysis:

- Tie rod (6061-T6): axial FOS 2.75, buckling FOS 1.41
- Custom clevis rod end (1144 steel): FOS 1.14 (realistic operating FOS ~10.4)
- Rack extensions (7075-T6): buckling FOS 4.0, <0.2 mm displacement

- Linear rail inserts designed to remove large moment arms + protect chassis paneling
- Rack & pinion mount validated for combined moment + compressive load with FOS ≥ 1.5

Failure-Avoidance Enhancements:

Added linear bearing rail system to eliminate bending moment transfer to chassis CF panels, and steering stops to limit rack travel and ensure reliability under realistic racing loads.

Impact

Delivered a structurally validated, competition-ready steering system with:

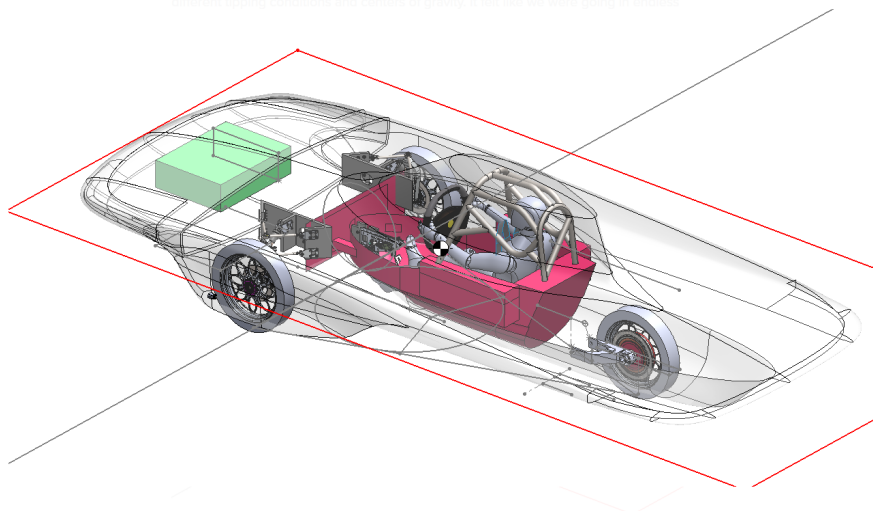
- Verified compliance with turning radius & geometry constraints from other subsystems
- Dramatically improved rigidity/simulations vs. the previous vehicle
- Reduced local rack mount panel stress and avoided historical failure modes from Gen-10
- Safer steering response under extreme driver load conditions
- Clear manufacturable drawings, BOM, and installation guidelines for team implementation and future generational knowledge transfer

Skills Demonstrated

- Steering system architecture & Ackermann geometry design
- Load case development + worst-case engineering safety evaluation
- Extensive FEA validation (buckling, combined load, joint stress, bolt preload analysis)
- CAD master assembly development & linkage parametric derivation
- Integration of steering + suspension constraints, including anti-bump steering preservation
- Mechanical design for manufacturability, reliability, and serviceability

2. Stability Analysis Tool

Detailed Critical Design Review Slidedeck (first 8 slides)



Objective

Developed a vehicle-level stability analysis tool to guide early architectural decisions for CalSol's 11th-generation solar vehicle, including track width, wheelbase, ground clearance, and mass distribution. The tool was designed to quantitatively verify static tipping safety while enabling rapid iteration across multiple, interdependent subsystems during early-stage vehicle layout.

Methodology

Defined stability functional ASC regulations and constraints

- No tipping when the vehicle is tilted 45° about an axis formed by any two wheels
- Minimum 104 mm ground clearance (regulation minimum: 100 mm)
- Compatibility with our trailer packaging constraints
- Steering geometry constraints: wheel angles < 25° while maintaining a 7.5 m turning radius

Integrated all major mass-dominant components

Using subteam-provided values (including worst-case mass uncertainties) and updated estimates:

- Roll cage, driver, pedal mount, seat belt system
- Steering wheel, battery, electrical system, solar array
- Rims & tires, motor, suspension components

Leveraged SolidWorks mass property calculations to dynamically compute center of gravity (CoG) as component placement, vehicle dimensions, and packaging evolved.

Evaluated tipping conditions using two criteria:

- Actual CoG height must be less than the distance from the CoG to the tipping axis formed by any two wheels
- Actual CoG height must be less than the maximum allowable geometric CoG

Geometric COG Constraint

Used a legacy trade-study calculator (developed by previous team members) to compute allowable CoG envelopes as a function of track width and wheelbase.

- For 1.55 m track width and 2.3 m wheelbase, maximum allowable CoG height: 21.92 in

Validated final subsystems configuration

- Actual CoG height: 18.88 in
- Distances to tipping axes: 19.79 in, 19.83 in, 28.51 in
- Result: tipping condition satisfied with 0.91 in vertical margin

Identified dominant contributors to CoG sensitivity, noting that roll cage and top shell had the largest negative influence on vertical stability margins, and the battery was our primary mode of shifting the COG forward

Impact

This tool served as the backbone for early vehicle architecture decisions, preventing isolated subsystem design that could compromise global stability. By centralizing mass properties and stability validation, the team avoided circular redesign loops, reduced unnecessary iteration time, and confidently locked in vehicle dimensions before committing to detailed subsystem designs. The model enabled cross-team alignment, ensured compliance with static stability requirements before hardware fabrication began, and defined the locations of mass-dominant items.

Skills Demonstrated

- Vehicle-level systems thinking and architectural trade studies
- Center-of-gravity modeling and static stability analysis
- CAD-driven mass property management and configuration control
- Cross-subsystem integration (chassis, suspension, steering, shell, electrical)
- Engineering decision support tooling and design bookkeeping for large teams

3. Bolt Preload Calculator/Bolted Connection Tutorial

The screenshot shows a spreadsheet-based bolt preload calculator. It includes sections for input parameters, results, and guidelines.

Input Parameters:

Parameter	Value	Units
Bolt Material # from Material Table	43	
Yield Strength, S_y	275.79	MPa
Thread Size	#10-32	-
Nominal Diameter, d_{nom}	4.83	mm
Tensile Stress Area, A_t	0.1290	cm ²
Preload % of Yield, $\% \text{ of Yield}$	66.7	%
Preload Coefficient, K_T	0.2	-
Preload Uncertainty, $\% \text{uncrt}$	25	%
Preload Relaxation, $\% \text{relax}$	10	%

Bolt Selection: Inch Metric

Results:

Preload Force, F_{PL} (N)	Install Torque, T (N·m)	% of Yield Strength	Torque Coefficient, K_T
2,373	2.2903	66.7	0.2

The nominal value is the design target, and the min and max values account for preload uncertainty and relaxation.

Preload Force (N):	Nominal	Minimum	Maximum
% of Yield Strength	66.7	1.542	2.966

Preload (% of Yield):

When to Use	Preload (% of Yield)	Notes
Conservative, moderate/variable loads	50%	Shigley/Lindberg recommendation
Balanced preload, general critical joints	60%	Safer with slightly better clamping
Rule of thumb, general use	66.70%	Common default, good balance
High preload, static-heavy joints	75%	Only if ductility & design allow
Max preload (proof strength)	85%	Beyond this risks plastic deformation
Avoid unless specialized application	>85%	Use only with testing or FEA

Torque Coefficient:

Bolt Condition	K_T
Nonplated, black finish	0.3
Zinc-plated	0.2
Lubricated	0.18
With Anti-Seize	0.12

Preload Uncertainty:

Tightening Method	Accuracy
By feel	±35%
Torque wrench	±25%
Turn-of-the-nut	±15%
Load indicating washer	±10%
Bolt elongation	±5%
Strain gages	±1%
Ultrasonic sensing	±1%

Preload Relaxation:
Preload loss allowance approximately 10% is sufficient as a general rule

Objective

Designed a bolt preload calculator and SolidWorks simulation tutorial to improve the accuracy and consistency of joint design across CalSol's mechanical systems. The goal was to eliminate undocumented torque assumptions, prevent unsafe over-preloading, and enable reliable bolted-joint simulation within SolidWorks FEA workflows.

Methodology

Developed a spreadsheet-based engineering tool that bridges analytical joint design and simulation:

Allowed users to input joint-specific parameters

- Bolt material and grade (e.g., SAE J429 Grade 8, Class 10.9, etc.)
- Thread size and pitch (metric or imperial)
- Torque coefficient based on surface condition (zinc-plated, dry, lubricated)
- Assembly method accuracy (torque wrench, turn-of-nut, etc.)
- Implemented a preload-as-percent-of-yield framework with clear guidelines

Easy to use output

Minimum, nominal, and maximum installation torque values (N·m) accounting for preload uncertainty and relaxation.

Integrated directly into the team's SolidWorks Simulation workflow by using calculated torque values as bolt preloads for combined loading analysis.

Documented Solidworks Tutorial

Complemented the calculator with easy-to-follow guidelines linked above to teach members how to properly model bolted connections and evaluate bolt Factor of Safety (FOS) under realistic loading conditions.

Impact

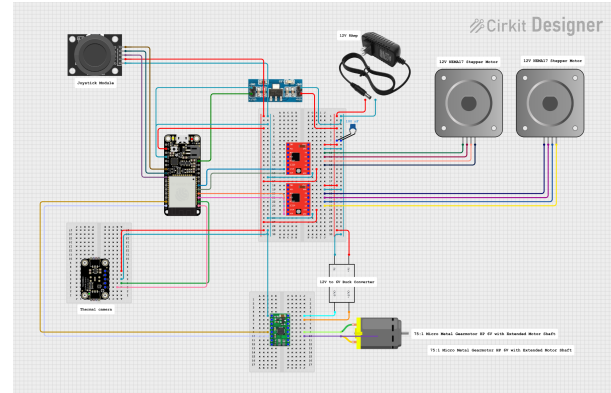
This tool standardized bolted-joint design across the team, replacing guess-based torque values with traceable, defensible engineering inputs. It reduced the risk of over-preloading, which can artificially lower bolt and part FOS in simulation while improving confidence in joint performance under real loading. The calculator also served as long-term documentation, enabling team members to design and simulate joints consistently across vehicle generations.

Skills Demonstrated

- Mechanical joint design and fastener mechanics ([Shigley](#) and [Machinery's Handbook](#) referenced)
- Preload selection, torque uncertainty, and yield-based design practices
- Integration of analytical tools with FEA workflows
- Development of reusable engineering tools for large teams
- Technical documentation and knowledge transfer

4. πRo-Bot: Autonomous Fire Suppression Robot

[YouTube Video Demo](#)



Objective

Designed and developed πRo-Bot, a compact, automated fire suppression system to detect, extinguish, and prevent brush fires. The system enhances real-time fire mitigation through infrared detection, remote accessibility, and preemptive deterrence in high-risk areas.

Methodology

πRo-Bot is an advanced, automated fire suppression system featuring a multi-modal control architecture for enhanced adaptability in wildfire-prone environments. It operates in three distinct modes:

- Automatic Mode: Utilizes a high-resolution infrared (IR) sensor array for real-time thermal imaging, detecting fire sources based on temperature thresholds. A closed-loop feedback system continuously adjusts the water jet trajectory for accurate suppression.
- Manual Mode: Implements a low-latency wireless control interface, allowing direct operator intervention via an off-the-shelf analog joystick controller. This mode ensures precise targeting in complex fire conditions.
- Preventive Mode: Integrates remote command protocols to autonomously spray fire retardant or water within a predefined area. The system features geofencing capabilities, enabling targeted preemptive fire prevention in high-risk zones

Impact

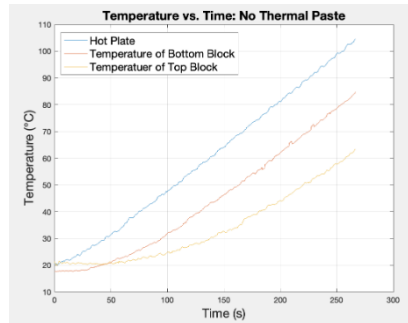
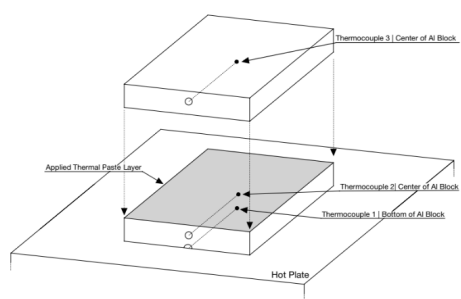
Addresses growing wildfire threats by providing a scalable, automated solution for fire suppression and prevention. Enhances firefighter safety by enabling **remote fire mitigation** in hazardous conditions. Offers a **cost-effective alternative** to traditional suppression methods, reducing response times and environmental damage.

Skills Demonstrated

- Embedded systems & automation for real-time fire detection and suppression.
- Infrared sensing & computer vision for precise heat-source targeting.
- Wireless control system design using game controllers for manual operation.
- Mechanical & electrical integration for a compact, mountable fire mitigation device.

5. Thermal Paste Performance Evaluation for Heat Transfer Optimization

[Full Report Available Here](#)



Objective

Investigated the thermal performance of different thermal pastes to enhance CPU/GPU cooling efficiency, ensuring optimal heat dissipation for high-performance computing applications.

Methodology

Designed a controlled experiment using custom-milled aluminum blocks, K-type thermocouples, an ESP32 microcontroller, and an insulating fiber blanket to measure heat transfer. Conducted calibration procedures with ice and boiling water for thermocouple accuracy. Tested Noctua NT-H2, Arctic MX-6, and Thermal Grizzly Kryonaut using a temperature-controlled hot plate to simulate real-world CPU heat generation.

Key Findings

Thermal Grizzly Kryonaut exhibited the best thermal conductivity, minimizing the temperature gradient and improving heat dissipation. Results aligned with third-party data, reinforcing the importance of thermal interface materials (TIMs) in cooling.

Impact

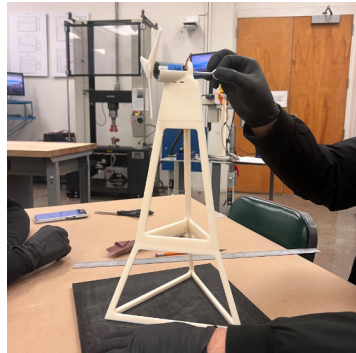
Provides engineers, PC builders, and overclocking enthusiasts with data-driven insights into selecting effective thermal pastes. Findings contribute to better heat management in consumer electronics and industrial applications, ensuring longevity and performance stability.

Skills Demonstrated

- Thermal system evaluation and experimental design
- Data acquisition and signal processing using thermocouples and microcontrollers
- MATLAB-based data analysis for trend validation and result interpretation
- Mechanical design and fabrication of precision-milled components
- Troubleshooting and optimization to improve measurement reliability

6. 3D Printed Wind Turbine Design and Testing

[Full Report Available Here](#)



Objective

Designed, 3D-printed, and tested a **miniature wind turbine** with the goal of **generating electricity** while ensuring structural stiffness and material efficiency.

Methodology

The wind turbine blade was designed using the NACA 4418 airfoil profile, with an optimized angle of attack (7.5°) and twist (15.3°) to enhance energy conversion efficiency. A three-blade configuration was selected to balance aerodynamic performance and structural stability. The tower structure was designed with a triangular support configuration, maximizing stiffness while minimizing material usage. The design adhered to weight and height constraints to ensure compatibility with testing conditions. To assess the tower's structural integrity, a Finite Element Analysis (FEA) was conducted, simulating stress distribution, deflection, and the safety factor under operational loads. This analysis allowed for refinements in geometry to enhance mechanical stability. The wind turbine's performance was evaluated through controlled experimental testing, measuring power output, deflection under applied loads, and wind speed. The setup provided real-world validation of the design, ensuring the turbine's effectiveness in generating electricity.

Key Findings

The turbine **produced a peak power output of 1.823 W**, slightly under the **2 W target** but demonstrated high efficiency (98.75%). The tower **achieved a stiffness of 14.2 N/mm**, exceeding the 8 N/mm requirement, with a **maximum deflection of 3.17 mm under a 5 kg load**. The wind speed test confirmed 24.5 mph airflow, allowing optimal blade rotation and power generation.

Impact

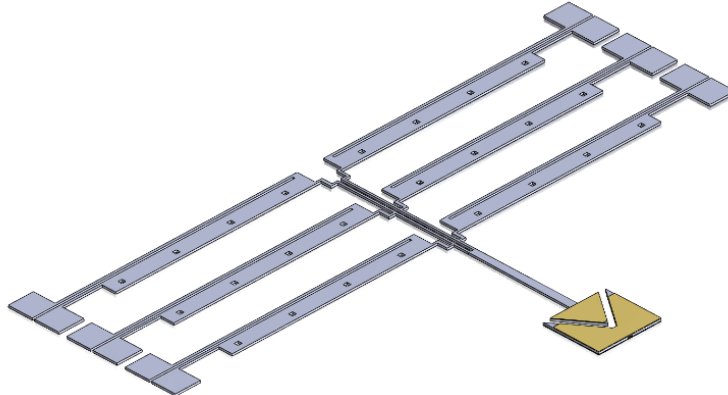
Provides insights into efficient wind turbine design for small-scale energy applications. Demonstrates 3D printing as a viable method for rapid prototyping and optimization in renewable energy projects. Offers a scalable approach for low-cost, custom-built wind energy solutions.

Skills Demonstrated

- 3D modeling and manufacturing using SolidWorks and 3D printing.
- Experimental data collection and validation for performance metrics.
- Optimization of mechanical structures for efficiency and material constraint

7. Microfluidic Exhaust Valve (**MUMPS**)

[Full Report Available Here](#)



Objective

Designed and analyzed a **microfluidic exhaust valve** utilizing **thermal actuator arrays** and **electrostatic latching** to enhance fluid control and minimize leakage in MEMS devices.

Methodology

Developed a **yoke-configured thermal actuator array**, adapted from Comtois and Bright (1997), to generate precise force for sealing microfluidic channels. Implemented an **electrostatic latching mechanism**, inspired by the Scratch Drive Actuator concept, using a gold-chromium metal layer to enhance sealing via voltage-controlled attraction. Ensured the device can be fabricated using the **MUMPS process**, ensuring compliance with MEMS design constraints.

Key Findings

The **thermal actuator array generated 93 μN** of force at 8 μm deflection, effectively sealing the channel. Electrostatic latching demonstrated potential for **further enhancing the seal**, with force scalability based on applied voltage. Identified **design challenges**, including wiring integration for thermal actuation and electrostatic control.

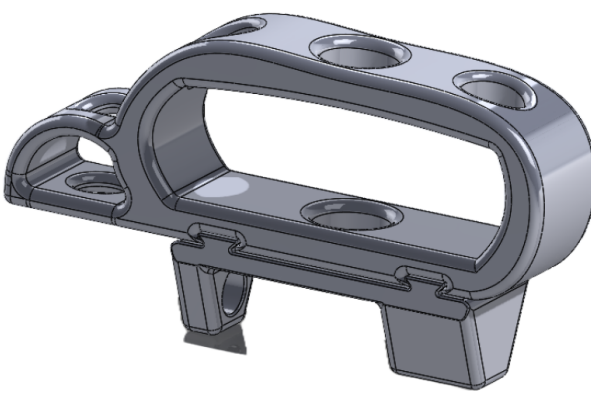
Impact

Provides a novel approach to **reducing leakage in microfluidic MEMS systems**, improving precision in applications like biomedical diagnostics and micro-robotics. Demonstrates the feasibility of combining thermal and electrostatic actuation for robust, electronically controlled fluidic devices.

Skills Demonstrated

- MEMS device design and microfabrication principles.
- Electrothermal actuation and electrostatics in fluidic control.
- Computational modeling and analysis for force estimation and sealing effectiveness.
- Microfluidic system integration and performance evaluation.

8. Assistive Utensil Device



Objective

Developed an ergonomic utensil assistive device designed to **enhance independence** for individuals with **limited finger mobility** due to musculoskeletal disorders, arthritis, or amputations.

Methodology

Designed a **flexible, palm-fitting band** to maximize **comfort, stability, and ease of use**. Created **interchangeable utensil adapters** using a **dovetail mechanism**, ensuring compatibility with different utensil types. Focused on **affordability** by utilizing **durable plastics and polymers** instead of metals.

Key Features

Designed to accommodate various hand sizes, ensuring a secure and ergonomic grip for maximum comfort and ease of use. By reducing strain on the fingers and joints, it effectively eliminates discomfort associated with traditional utensil use for individuals with limited finger mobility. The device is highly customizable and amputee-friendly, allowing users to adapt it to their specific needs for greater usability and independence. Additionally, it is printed with TPU (SLA) which is durable yet cost-effective, ensuring long-term daily use without the need for expensive components.

Impact

Restores independence in dining for individuals with limited mobility. Reduces pain and the need for painkillers, improving overall quality of life. Potential health benefits, including lower stress and blood pressure, which may contribute to increased life expectancy.

Skills Demonstrated

- Human-centered design for accessibility solutions.
- Ergonomic product development with adaptive mechanics.
- Rapid prototyping and material selection for cost-effective manufacturing.
- Problem-solving for mobility impairments through iterative testing and user feedback

9. SolarSync: Automated Window Blinds

Objective

Developed an **automated window blind system** that adjusts based on external sunlight levels to improve **sleep-wake cycles** and energy efficiency.

Methodology

Integrated a photoresistor sensor to detect ambient light levels. Utilized an **ESP32 microcontroller** for real-time data processing and control. Implemented a **DC motor** with an **H-Bridge driver** for smooth actuation of the blinds. Enabled **wireless data transmission** using ESP-NOW, ensuring efficient and responsive operation.

Key Features

The photoresistor sensor was carefully tuned to accurately detect natural light variations, minimizing false positives and ensuring reliable performance. A software-based tracking system was implemented to monitor open and closed states, allowing the blinds to adjust automatically without manual intervention. To achieve precise and smooth movement, motor tuning techniques were tested and optimized, preventing excessive power consumption and mechanical strain. The system operates on a 3.7V Li-ion cell, utilizing a deep sleep state to enhance energy efficiency and ensure sustainable, low-power operation.

Impact

Enhances circadian rhythm regulation, leading to better sleep quality by aligning light exposure with natural sleep cycles. Provides cost-effective automation, offering a more affordable alternative to existing smart blind systems. Reduces energy consumption by optimizing natural light usage, potentially lowering electricity costs.

Skills Demonstrated

- Embedded systems development using ESP32 and ESP-NOW.
- Sensor integration for ambient light detection and motorized actuation.
- Software design for state tracking and automation logic.
- Hardware prototyping and motor control optimization.